JOURNAL OF COMPUTATIONAL PHYSICS **83**, 361–372 (1989)

An Energy-Minimizing Mesh for the Schrödinger Equation

ZACHARY H. LEVINE* AND JOHN W. WILKINS*

Laboratory of Atomic and Solid State Physics,
Cornell University, Ithaca, New York 14853-2501

Received April 1, 1988; revised October 21, 1988

A formula is derived which gives the optimum placement of mesh points in the sense of minimizing the error in energy for a given number of degrees of freedom. The wave function is assumed to be given in a finite difference or finite element representation with polynomial completeness to an arbitrary but fixed degree. The result depends explicitly on the wave function, the kinetic energy operator, and the degree of polynomial completeness for the representation but does not depend explicitly on the potential, even in the presence of a Coulomb singularity. The optimum mesh predicted here for the hydrogen atom is compared to the widely used Herman–Skillman mesh. A 1-dimensional example is given in which the calculated error in energy displays a sharp minimum at the predicted optimal mesh density. The critical role of reproducing the analytic structure of the solution is illustrated with an additional example in one dimension. The hydrogen $1s$ wave function is considered as a 3-dimensional problem, and an optimal mesh density is calculated. A singular mesh density is required to account for the cusp while retaining the convergence properties of the basis set. A few percent of the available degrees of freedom are devoted to the description of the wave function cusp in the optimal mesh.

1. INTRODUCTION

The numerical solution of the Schrödinger equations has been a subject of study since the work of Hartree [1]. Computer solutions of atomic energy levels using Slater's X-α approximation [2] were performed extensively by Herman and Skillman [3] in the early 1960s. Owing to the change in the natural scale length for the wave functions as a function of distance from the nucleus, Herman and Skillman adopted a mesh whose step size doubles at certain pre-determined internal locations. While practical, no claim is made for optimality in this approach which in any event is not critical for the atomic problem.

Larger systems are typically treated with a basis set. Molecules are usually treated with Gaussian orbitals [4], whereas for solid state problems, plane waves are often employed with norm-conserving pseudopotentials [5], or with an additional angular-momentum basis set near the nuclei [6]. The successes of these

---

* Present address: Department of Physics, The Ohio State University, Columbus, Ohio 43210.

0021-9991/89 $3.00

methods are numerous [7]. However, in evaluating their limitations, it is often difficult to disentangle the issues of the quality of the numerical approximations, the quality of the pseudopotentials, and the limitations of the local density approximation (LDA) itself [8].

Quite recently, some workers have begun pilot investigations using the finite element method in the description of electronic structure [9–14] and reactive scattering [15, 16] problems. With a finite element basis, one may arrive at a numerical scheme in which the time to find a wave function grows linearly in the number of basis functions retained through the use of multigrid techniques [17]. Recent advances in numerical techniques, have permitted pseudopotential-based plane wave calculations to perform nearly this well [5, 18]. A finite element basis allows a fine variation of the spatial density of the degrees of freedom which may permit all electron calculations or the use of deep local pseudopotentials on systems of substantial size. One hope is that highly converged properties such as energies, may become available through the use of finite elements. Another motivation for introducing finite elements into quantum mechanical calculations is to treat finite and extended systems on the same footing.

The number of finite element basis functions required for a realistic electronic structure calculation presently required is sufficiently large to represent an obstacle in the practical realization of this method. This work addresses that issue by providing an explicit formula for an optimal mesh point placement for electronic structure problems in the sense of minimizing the energy. Some 1-dimensional examples are given to demonstrate the validity of the formula and to gain insight into its implications for a general electronic structure calculation. Through optimal or near-optimal mesh point placement, the convergence rate of the energies as function of the basis set size can avoid the degradation in accuracy that the wave function cusp at the nucleus would impose if a uniform mesh were used. Rapid convergence for the energies is not only important in its own right, but also necessary to ensure the quality of the wave function for the purpose of computing expectation values of unbounded operators, such as the dipole or higher moments of the charge distribution [19].

2. VARIATIONAL OPTIMIZATION OF MESH DENSITY

Let $\rho(\mathbf{r})$ be the number density of mesh points at a given point of space, where the number of mesh points is taken as sufficiently large so that a continuum description is appropriate. The mesh density is constrained by the total number of mesh points in the space M, i.e.,

$$\int d\mathbf{r}\, \rho(\mathbf{r}) = M. \tag{2.1}$$

Suppose we wish to minimize some functional of $\rho(\mathbf{r})$

$$I = \int d\mathbf{r}\, \varepsilon(\mathbf{r})\, f(\rho(\mathbf{r})), \tag{2.2}$$

where $f(\rho)$ is some positive function for which the inverse of its derivative (f'^{-1}) exists and $\varepsilon(\mathbf{r})$ is another positive function referred to as the "penalty function." To minimize I subject to the constraint of Eq. (2.1), we introduce the Lagrange multiplier λ and minimize the modified functional

$$\tilde{I} = \int d\mathbf{r}\, \varepsilon(\mathbf{r})\, f(\rho(\mathbf{r})) + \lambda \int d\mathbf{r}\, \rho(\mathbf{r}), \tag{2.3}$$

with respect to variations in the function ρ and the scalar λ.

In general, this minimization yields

$$\rho(\mathbf{r}) = f'^{-1}\left(-\frac{\lambda}{\varepsilon(\mathbf{r})}\right), \tag{2.4}$$

where λ is determined from this expression and Eq. (2.1). If $f(\rho) = \rho^{-\alpha}$, then

$$\rho(\mathbf{r}) = M \frac{\varepsilon(\mathbf{r})^{1/(\alpha+1)}}{\int d\mathbf{r}\, \varepsilon(\mathbf{r})^{1/(\alpha+1)}}. \tag{2.5}$$

As indicated below, α will be related to the truncation error of the representation. A penalty function for which $\int d\mathbf{r}\, \varepsilon(\mathbf{r})^{1/(\alpha+1)}$ is unity is said to be "normalized." The problem of a variationally determined mesh has been discussed elsewhere for a variety of cases [20].

In a typical solution to the Schrödinger equation, several orbitals are determined on the same mesh. It is reasonable (but not necessary) to require that the penalty function $\varepsilon(\mathbf{r})$ be given by the sum of the normalized penalty functions associated with the individual orbitals. In the case where the mesh densities $\rho_1(\mathbf{r}), ..., \rho_k(\mathbf{r})$ are known for a set of k orbitals, the total mesh density will be given by the combination rule

$$\rho_{\text{tot}}(\mathbf{r}) = M \frac{(\sum_{i=1}^{k} \rho_i(\mathbf{r})^{\alpha+1})^{1/(\alpha+1)}}{\int d\mathbf{r} (\sum_{i=1}^{k} \rho_i(\mathbf{r})^{\alpha+1})^{1/(\alpha+1)}}. \tag{2.6}$$

For large α, this combination rule is nearly the same as choosing the maximum ρ at each point in space, then renormalizing.

3. AN OPTIMAL MESH DENSITY

For the Schrödinger equation, let $\psi(\mathbf{r})$ be the best solution which is representable by a given basis set, and let $\psi_0(\mathbf{r})$ be the exact normalized solution with energy E_0. Define the error term $\delta\psi(\mathbf{r})$ by

$$\psi(\mathbf{r}) = \psi_0(\mathbf{r}) + \delta\psi(\mathbf{r}), \tag{3.1}$$

and note the orthogonality condition $\langle \psi_0 \mid \delta\psi \rangle = 0$. Deviation of the Rayleigh quotient for $\psi(\mathbf{r})$ from the exact energy E_0 is given by

$$\delta E = E - E_0 = \frac{\langle \psi | \, H - E_0 \, | \psi \rangle}{\langle \psi \mid \psi \rangle}$$

$$= \langle \delta\psi | \, H - E_0 \, | \delta\psi \rangle + O(\delta\psi^4). \tag{3.2}$$

Suppose the function $\psi(\mathbf{r})$ has an expression in terms of a finite element basis set with polynomial completeness through order N. Suppose further that $\psi_0(\mathbf{r})$ is differentiable through at least Nth order, except at isolated points (i.e., Coulomb singularities). Decomposing $H = T + V$ into the usual kinetic energy and potential terms, the discussion of Strang and Fix [21] may be specialized to say

$$\langle \delta\psi | \, T \, | \delta\psi \rangle \leqslant C_T h^{2N} \, |\psi_0|^2_{N+1} \tag{3.3}$$

and

$$\langle \delta\psi | \, V - E_0 \, | \delta\psi \rangle \leqslant C_V h^{2(N+1)} \, |\psi_0|^2_{N+1}. \tag{3.4}$$

Here, h is the scale length for the size of the individual finite elements, and C_T and C_V are constants which may depend on H, E, $\rho(\mathbf{r})$, and the discretization rule [22], but not on h; $|\psi_0|_{N+1}$ is the seminorm defined by

$$|\psi_0|^2_{N+1} = \sum_{|\beta| = N+1} \int_\Omega d\mathbf{r} \, |D^{\beta_1 \cdots \beta_d} \psi_0(\mathbf{r})|^2, \tag{3.5}$$

where Ω is the domain of integration, d is the dimension of the space, and D is the partial differential operator defined by $D^{\beta_1 \cdots \beta_d} = \partial^{|\beta|} / (\partial^{\beta_1} \cdots \partial^{\beta_d})$ with $|\beta| = \beta_1 + \cdots + \beta_d$. All derivatives of order exactly $N+1$ are included in the summation. Attention is directed to minimizing the error in kinetic energy, as it will always dominate for sufficiently small h. Remarkably, the presence of isolated singularities in the exact solution $\psi_0(\mathbf{r})$ will not affect the estimates of the rate of convergence of the matrix elements in Eqs. (3.3) and (3.4) if the mesh is sufficiently dense near the singularities [23].

Consider the division of the total region of integration into small domains $\Omega_1 \cdots \Omega_K$ for some large integer K. The error in the kinetic energy (Eq. (3.3)) for each locally defined domain is given by the seminorm Eq. (3.5) for which the region of integration Ω_j is small, and hence given approximately by the integrand of Eq. (3.5). Hence, to the extent that the error bound given by Eq. (3.3) is optimal, the choice of the penalty function

$$\varepsilon(\mathbf{r}) = \sum_{|\beta| = N+1} |D^{\beta_1 \cdots \beta_d} \psi_0(\mathbf{r})|^2 \tag{3.6}$$

is also optimal. The associated error is $O(h^{2N})$, so $h^{2N} = f(\rho)$. Since $\rho(\mathbf{r}) \sim h(\mathbf{r})^{-d}$,

$f(\rho)=\rho^{-2N/d}$, i.e., $\alpha=2N/d$. This set of choices leads to the mesh density via Eq. (2.5)

$$\rho_{\mathrm{opt}}(\mathbf{r})\sim\Bigg(\sum_{|\beta|=N+1}|D^{\beta_1\cdots\beta_d}\psi_0(\mathbf{r})|^2\Bigg)^{1/(2N/d+1)}. \tag{3.7}$$

In one dimension, the sum reduces to the single term

$$\rho_{\mathrm{opt}}(x)\sim\left|\frac{\partial^{N+1}}{\partial x^{N+1}}\,\psi_0(x)\right|^{1/(N+1/2)}. \tag{3.8}$$

Although the optimum mesh density depends explicitly on the solution, a coarse-grained solution suffices to estimate ρ_{opt}. Strategies are emerging to solve equations on a solution-dependent mesh in two or three times the time required for obtaining the solution on a mesh which is fixed in advance [24, 25].

4. ONE-DIMENSIONAL EXAMPLES

Herman–Skillman Mesh

It is interesting to compare the result of Eq. (3.8) to the mesh employed in the extensive atomic calculations of Herman and Skillman. Consider the ground state solution to the hydrogen radial equation ($u(r)\equiv r\psi_{1s}(\mathbf{r})$)

$$u(r)=re^{-r}, \tag{4.1}$$

where atomic units are used. Application of Eq. (3.8) leads to the (unnormalized) mesh densities

$$\rho_{\mathrm{opt}}(r)\sim|r-(N+1)|^{1/(N+1/2)}\,e^{-r/(N+1/2)}. \tag{4.2}$$

Herman and Skillman [3] employed the Numerov method [26], for which $N=5$. The Herman–Skillman mesh is roughly logarithmic between its starting and ending points. Equation (4.2) is well defined at the origin and integrable over the full range 0 to ∞. Thus Eq. (4.2), combined with a simple discretization rule [22], will provide a definite prescription for the location of the outermost mesh point for a given total number of allowed points.

Figure 1 compares the Herman–Skillman mesh for the hydrogen atom and the result stated in Eq. (4.2). Herman and Skillman wished to use the same mesh for all atomic orbitals (except for a scale factor of $Z^{1/3}$), hence they required the additional mesh points at small r and large radii for certain orbitals. Thus their mesh density must necessarily fall below our 1s-derived $\rho(r)$ at intermediate r. To model a typical heavy atom, optimal meshes were found from Eq. (3.8) for the four lowest s states of the hydrogen atom. The meshes were combined using the rule of

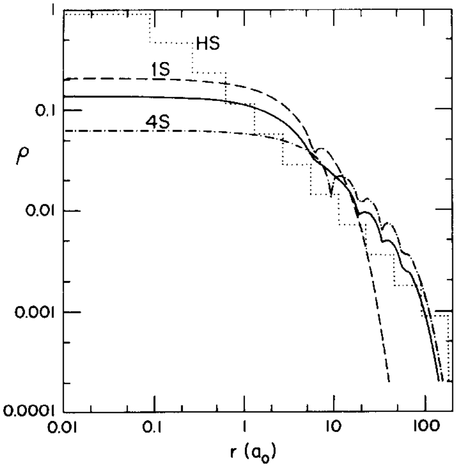

FIG. 1. Mesh density for the hydrogen atom as a 1D problem. The mesh density is normalized to $\int_0^\infty dr\, \rho(\mathbf{r}) = 1$. Dotted curve is the Herman–Skillman mesh [3]. Dashed curve is normalized optimum formula for the hydrogen 1*s* orbital described by the Numerov method (Eq. (4.2) with $N = 5$). The dash–dot curve is the analogue for the hydrogen 4*s* orbital. The mesh densities for the 2*s* and 3*s* orbitals generally lie between the curves associated with 1*s* and 4*s* orbitals, but are suppressed for clarity. The solid curve is the optimum mesh formula based on a combination of the first four hydrogen *s*-orbitals.

Eq. (2.6) to obtain the solid line in Fig. 1 which agrees well with the empirically optimized Herman–Skillman mesh. The major discrepancy for small *r* may be understood by noting that in heavy atoms the effective charge is larger in the core than the valence region, hence the range of scale lengths to be treated is somewhat larger than for hydrogen.

δ-Functional Potential

The potentially critical role that mesh point optimization may play in a practical calculation is illustrated by a numerical experiment. The eigenvalues are found for an exponential wave function arising from a δ-function potential. In the case considered, the wave function was confined to a box with walls at $\pm 10 a_0$ and an attractive potential in the center of sufficient strength so that the ground state energy was $-1\,Ry$. The ground state wave function

$$\psi_0(x) = e^{-|x|} \tag{4.3}$$

is associated with the mesh density function

$$\rho_{\text{opt}}(x) = e^{-|x|/(N+1/2)}. \tag{4.4}$$

This optimal expression may be generalized to

$$\rho(x) = e^{-|x|/x_0} \tag{4.5}$$

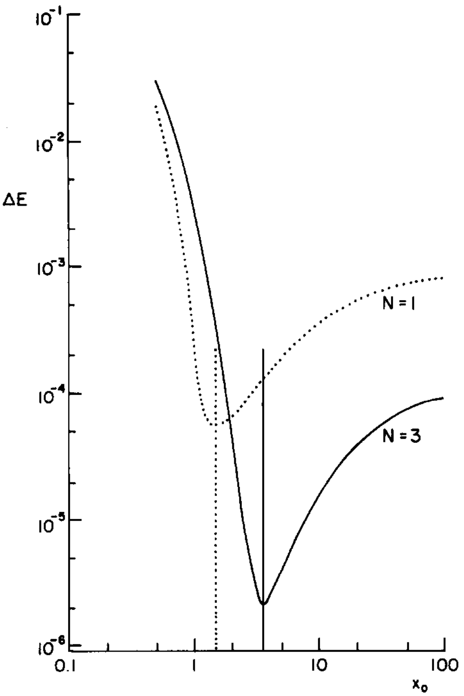

FIG. 2. Eigenvalue excess (ΔE) for exponentially decaying wave functions in one dimension versus exponential parameter (x_0) for mesh density function. Solid curve is for $N = 3$, and dotted curve is for $N = 1$. Vertical bars represent predicted optimal values.

to introduce a parameter (x_0) which is expected to achieve an optimal value at $x_0 = N + \frac{1}{2}$. Energy eigenvalues were found for a finite element calculation using linear Hermite polynomials (for which $N = 1$) and cubic Hermite polynomials (for which $N = 3$) [27]. Figure 2 illustrates the error in energy for $N = 1$ with 199° of freedom and $N = 3$ with 28° of freedom. It is seen that the calculated excess in the energy eigenvalue has a sharp minimum at the predicted optimal mesh density (i.e., $x_0 = \frac{3}{2}$ and $\frac{7}{2}$, respectively).

Square-Well Potential

We studied approximations to the lowest eigenstate in a one dimensional square-well potential of length πa_0. The exact wave function is proportional to $\sin x$ with an eigenvalue of $1\,Ry$. We considered finite element solutions for $N = 1$ elements with 100° of freedom and for $N = 3$ with 16° of freedom. The meshes were taken to be in the forms $|\sin x|^{\alpha}$, $|\cos x|^{\alpha}$, and $|\sin 2x|^{\alpha}$. (The uniform mesh is the $\alpha = 0$ limit in all cases.) The first form is densest in the middle where the wave function is largest, the second at the edges where the slope of the wave function is largest, and the third is maximal where the product of slope and value is maximal. Equation (3.8) predicts that the form $|\sin x|^{\alpha}$ is the optimal form for odd N. We observed that the $|\sin x|^{\alpha}$ mesh lowered the eigenvalues compared to the uniform mesh for all exponents studied, namely $\alpha = 0$ to 1, with a quadratic minimum appearing near the predicted value. Results are reported in Table I. The other two forms of the mesh density always yielded energies higher than the uniform value, with the $|\cos x|^{\alpha}$ mesh yielding a worse estimate than the $|\sin 2x|^{\alpha}$ mesh for equal value of α. A monotonic increase with α was observed in both cases. The form of the optimal mesh is correctly predicted by Eq. (3.8). The modest discrepancy in the optimal value for the $N = 3$ case may be due to the fact that Eq. (3.8) was derived on the assumption of a large number of intervals, whereas only a few (8) are used here. The energy at the predicted optimal value is within 10% of the observed optimum, as reported in the table. (Since the finite element method is variational, the calculated eigenvalues must lie above the exact value.) Although the improvements in this example are modest, it is instructive that the present theory correctly predicts optimization is possible even in the absence of a variation in the potential. A theory which predicts an optimized mesh only from the potential [28], however meritorious it may be in other ways, would not be capable of making such a prediction.

Effect of a Cusp

In the example of the δ-function potential, care was taken to place one of the $N = 1$ mesh points at the singularity in the potential and a very small interval was centered at the singularity in the $N = 3$ case. This is necessary to ensure the basis set is capable of correctly reproducing the analytic behavior of the solution (i.e., a cusp) at the singularity. In Fig. 3, the role of the failure to reproduce analytic behavior is illustrated. We present the results of calculations for the eigenvalue excess in the case of the uniform mesh for the square well and for the δ-function potential. In the case of the square well, the eigenvalue excess is seen to decline as n^{-2} for $N = 1$ and as n^{-6} for $N = 3$ where n is the number of degrees of freedom (i.e., the number of mesh points for $N = 1$, and twice the number of mesh points for $N = 3$, which has two functions per node). The functional form of this decline is

TABLE I

Optimal Mesh for a Uniform Potential

	$N=1$		$N=3$	
Mesh	α	$\Delta E(10^{-3})$	α	$\Delta E(10^{-7})$
Uniform	0	3.2	0	1.15
Observed optimal	0.65	2.4	0.31	0.72
Predicted optimal	$\frac{2}{3}$	2.4	$\frac{2}{5}$	0.78

Note. Results of a computer experiment on mesh optimization. The functional form of the mesh density is $|\sin x|^{\alpha}$. ΔE is the computed excess energy at the corresponding value of α; the exact eigenvalue is unity. The results for $N = 1$ had 100° of freedom, and the $N = 3$ results had 16° of freedom.

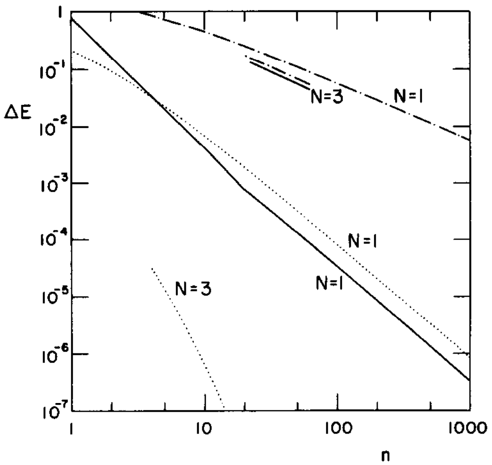

FIG. 3. Eigenvalue excess (ΔE) versus number of degrees of freedom (n) for various cases. Dotted lines are for the square-well problem; solid lines are for the δ-function potential with a mesh point at the singularity; chain dotted lines are for the δ-function potential without a mesh point at the singularity. The results are for $N=1$ and $N=3$ as indicated on the figure.

suggested theoretically and required for the argument of Section 3. When the uniform mesh is applied to the δ-function problem, the eigenvalue excess is seen to decline as n^{-1} for $N=1$ when no mesh point is placed on the singularity and with the same rate $N=3$ regardless of whether or not a mesh point is placed on the singularity. However, for $N=1$ with a mesh point at the singularity, the full n^{-2} behavior is observed. Only in this case is the approximate function free to have a discontinuity in slope just where the exact solution does; i.e., it has the correct analytic behavior. In the cases in which the slope discontinuity is not taken into account, i.e., mismatched function forms and no mesh grading, the rate of convergence is seen to be slow and independent of the order of the approximating polynomials.

5. EFFECT OF A NUCLEAR CUSP

The nuclear cusp poses a formidable obstacle to the calculation of 3-dimensional wave functions regardless of the numerical or physical approxiamtions chosen. The problem manifests itself in the present context as follows: in the finite element method, polynomials up to some specified degree (N) may be fit exactly. The (prototypical) hydrogen 1*s* wave function

$$\psi_{1s}(\mathbf{r}) = e^{-r} \tag{5.1}$$

may not be easily approximated by polynomials near the origin, as it depends upon $r=(x^2+y^2+z^2)^{1/2}$. The use of a uniform mesh under these circumstances would cause a substantial sacrifice of the convergence properties: convergence in energy would be limited to $O(h^{3/2})$ regardless of the choice of N rather than $O(h^{2N})$ which would obtain if the wave function were non-singular [29]. With appropriate mesh grading, the more rapid convergence is achieved. Application of Eq. (3.7) to ψ_{1s}, followed by spherical averaging, leads to an expression of the form

$$\rho_{\text{opt}}(\mathbf{r}) = \left(e^{-2r} \sum_{k=0}^{2N} c_k r^{-k} \right)^{-3/(2N+3)}, \tag{5.2}$$

for some coeficients c_k. Values for c_k are given in Table II for N up to 5, and the integrals of ρ_{opt} are plotted in Fig. 4. For small r, ρ_{opt} has an integrable singularity

$$\rho_{\text{opt}}(\mathbf{r}) \sim r^{-6N/(2N+3)}. \tag{5.3}$$

As N grows large, the mesh points are more concentrated at the nucleus and more mesh points are available at large radius. In the limit $N \to \infty$, the integrand mesh density diverges logarithmically near the nucleus. Recall that no singularity in mesh density was introduced for the atomic problem considered in Section 4; the cusp arising from the nuclear charge is hidden when the hydrogen wave function is described in terms of the variable r, which is not an analytic function of x, y, and z.

In practice, finite element calculations proceed with relatively low order elements. Typically N is chosen to be in the range 1 to 3, although N at least as large as five has been used in electronic structure calculations [11]. Figure 4 suggests that devoting 1–5% of the mesh points to the cusp region (say $r \leqslant 0.1$) is sufficient to prevent the non-analytic behavior at the nucleus from dominating the convergence

TABLE II

Optimal Mesh Coefficients for the Hydrogen Atom as a 3D Problem

N	1	2	3	4	5
A	25.191	412.86	648.82	1797.9	3697.1
C_0	4	64	52	423	2224
C_1	−2	−78	−102	−1286	−9018
C_2	9	267	363	2875	16789
C_3		690	1416	16506	117740
C_4		345	4164	79293	733430
C_5			5184	292512	3917040
C_6			2592	611136	16879920
C_7				697320	49186500
C_8				348660	91604250
C_9					100516500
C_{10}					50258250

Note. Coefficients are given for Eq. (5.2) for small N with $c_k = C_k/A$. The optimal mesh densities are plotted in Fig. 3. The C_k are integers, but trailing zeroes are not significant figures for $N = 4 - 5$.

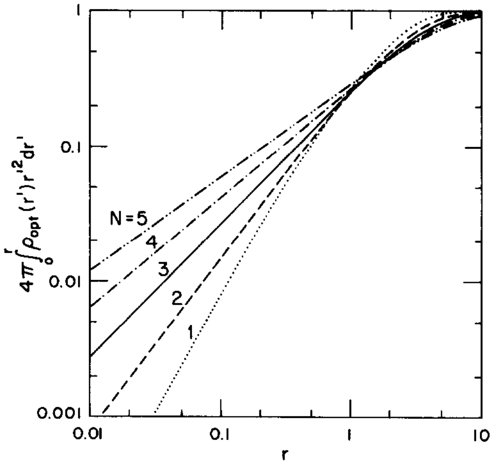

FIG. 4. Integrated normalized mesh density function for the hydrogen 1*s* wave function treated as a 3D problem versus radius. The function is determined by Eq. (5.2) with coefficients in Table I. Chain double dotted curve is for $N = 5$, chain dotted curve is for $N = 4$, solid curve is for $N = 3$, dashed curve is for $N = 2$, and dotted curve is for $N = 1$.

properties of the solution process. Outside the cusp region, the finite element solution is expected to be efficient. Beyond forcing the introduction of mesh grading, the nuclear cusp does not impose major computational costs.

It is of interest to consider qualitatively the characteristics of optimal meshes for general atoms in molecules or solids. The innermost core electron is nearly hydrogenic, so the analysis given here applies to it. For the succeeding shells (i.e., 2*s* and 2*p* and so on) the wave functions will show rapid variation in the region in which mesh points have been previously placed for inner shells, and a slow variation over a larger spatial region. Each additional shell will require roughly the same number of additional mesh points as the innermost shell, suggesting the representation of the full set of orbitals from an element such as copper or germanium will require only four times as many mesh points as the hydrogen 1*s* wave function.

ACKNOWLEDGMENTS

We thank Michael Teter and Steve White for stimulating discussions. Support from Department of Energy-Basic Energy Sciences, Division of Materials Research is gratefully acknowledged.

REFERENCES

1. D. R. HARTREE, *Proc. Cambridge Phil. Soc.* **24**, 89 (1927); D. R. HARTREE, *The Calculation of Atomic Structures* (Pergamon, New York, 1957).
2. J. C. SLATER, *Phys. Rev.* **81**, 385 (1951).
3. F. HERMANN AND S. SKILLMAN, *Atomic Structure Calculations* (Prentice–Hall, Englewood Cliffs, NJ, 1963); J. C. SLATER, *The Quantum Theory of Matter* (McGraw–Hill, New York, 1968), Chap. 7.

4. A Guassian orbital implementation of the X-α scheme is given by B. I. Dunlop, J. W. D. Connolly, and J. R. Sabin, *J. Chem. Phys.* **71**, 3396, 4493 (1979).
5. D. C. Allan and M. P. Teter, *Phys. Rev. Lett.* **59**, 1136 (1987) is a sample recent calculation with introductory comments reviewing recent developments in this area.
6. J. F. Janak and A. R. Williams, *Phys. Rev. B* **23**, 6301 (1981).
7. S. Lundqvist and N. H. March (Eds.), *Theory of the Inhomogeneous Electron Gas* (Plenum, New York, 1983).
8. The X-α approximation evolved into the more soundly based local density approximation of Hohenberg, Kohn, and Sham without significant change from a numerical point of view, P. Hohenberg and W. Kohn, *Phys. Rev.* **136**, B864 (1964); W. Kohn and L. J. Sham, *Phys. Rev.* **140**, A1133 (1965).
9. A. Askar, *J. Chem. Phys.* **62**, 732 (1975) is the earliest finite element study in quantum mechanics of which we are aware.
10. W. Schulze and D. Kolb, *Chem. Phys. Lett* **122**, 271 (1985).
11. D. Heinemann, D. Kolb, and B. Fricke, *Chem. Phys. Lett.* **137**, 180 (1987).
12. W. K. Ford and F. S. Levin, *Phys. Rev. A* **29**, 43 (1984).
13. F. S. Levin and J. Shertzer, *Phys. Rev. A* **32**, 3285 (1985).
14. S. R. White, J. W. Wilkins, and M. P. Teter, *Phys. Rev. B* **39**, 5819 (1989).
15. R. Jaquet, *Theor. Chim. Acta* **71**, 425 (1987) and references therein.
16. R. Kozak and F. S. Levin, *Phys. Rev. C* **36**, 883 (1987).
17. W. Hackbusch, *Multi-Grid Methods and Applications* (Springer-Verlag, Berlin, 1985).
18. R. Car and M. Parrinello, *Phys. Rev. Lett.* **55**, 2471 (1985). For these calculations and those in Ref. [5] the time to solution scales like $N_{\text{occ}} N_G \ln N_G$, where N_{occ} is the number of occupied states, and N_G is the number of plane waves retained in the calculation.
19. B. Klahn and J. D. Morgan III, *J. Chem. Phys.* **81**, 410 (1984).
20. See, for example, J. F. Thompson, Z. U. A. Warsi, and C. W. Mastin, *Numerical Grid Generation* (North-Holland, New York, 1985), Sect. IX.3.
21. G. Strang and G. J. Fix, *An Analysis of the Finite Element Method* (Prentice–Hall, Englewood Cliffs, NJ, 1973), pp. 106, 139.
22. Some rule for centering a set of M points in M small regions of space for which $\int \rho(\mathbf{r})\, d\mathbf{r} \approx 1$ in each region must be added to generate a particular mesh from the mesh density function. The regions must have a reasonably compact shape, containing a sphere of radius equal to $vh\rho(\mathbf{r})^{1/d}$, where v is a fixed constant. See Ref. [21, p. 139].
23. Ref. [21, pp. 155–156, 268].
24. E. L. Allgower and K. Bohmer, *SIAM J. Num. Anal.* **24**, 1335 (1987).
25. K. Eriksson and C. Johnson, *Math. Comput.* **50**, 361 (1988).
26. B. Numerov, *Publ. Observ. Cent. Astrophys. Russ.* **2**, 188 (1933).
27. See, for example, O. C. Zienkiewicz, *The Finite Element Method*, 3rd ed. (McGraw–Hill, London, 1977), p. 261. The linear Hermite functions have one degree of freedom per node and vanish at the endpoints of given intervals. The cubic Hermite functions have two degrees of freedom per node, one associated with the function value, and a second with the derivative. Each function and its derivative vanish at the ends of the intervals on which they are defined. The Hermite polynomials of the finite element method are distinct from the Hermite polynomials associated with the harmonic oscillator wave functions.
28. I. P. Hamilton and J. C. Light, *J. Chem. Phys.* **84**, 306 (1986).
29. Ref. [21, p. 155].